Experimental investigation of initial system-environment correlations via trace-distance evolution

Andrea Smirne,[1,2,*] Davide Brivio,[1,†] Simone Cialdi,[1,2,‡] Bassano Vacchini,[1,2,§] and Matteo G. A. Paris[1,3,‖]

[1]*Dipartimento di Fisica, Università degli Studi di Milano, Via Celoria 16, I-20133 Milan, Italy*

[2]*INFN, Sezione di Milano, Via Celoria 16, I-20133 Milan, Italy*

[3]*CNISM, Udr Milano, I-20133 Milan, Italy*

(Received 2 May 2011; published 16 September 2011)

The trace distance between two states of an open quantum system quantifies their distinguishability and, for a fixed environmental state, can increase above its initial value only in the presence of initial system-environment correlations. We provide experimental evidence of such a behavior. In our all-optical apparatus, we exploit spontaneous parametric down conversion as a source of polarization entangled states and a spatial light modulator to introduce in a general fashion correlations between the polarization and the momentum degrees of freedom, which act as environment.

DOI: 10.1103/PhysRevA.84.032112 PACS number(s): 03.65.Yz, 03.65.Ta, 42.50.Dv, 42.50.Ex

I. INTRODUCTION

The dynamics of an open quantum system S interacting with an environment E is usually described by means of a completely positive trace preserving (CPT) map on the state space of the open system [1]. The very existence of such a map generally requires that the initial correlations between the open system and the environment can be neglected, i.e., $\rho_{SE}(0) = \rho_S(0) \otimes \rho_E(0)$, where $\rho_S(0) = \mathrm{Tr}_E\{\rho_{SE}(0)\}$ and $\rho_E(0) = \mathrm{Tr}_S\{\rho_{SE}(0)\}$. However, this assumption is not always physically justified, especially outside the weak-coupling regime [2]. Therefore, different approaches to the description of the reduced system dynamics in the presence of initial correlations have been developed in recent years [3–8].

An approach for the study of initial correlations that is based on the use of the trace distance and that does not rely on the determination of any reduced dynamical map has been introduced in [9]. In particular, one can find a clear signature of initial system-environment correlations as follows: If the environmental state is fixed, the trace distance between any two reduced states can increase over its initial value only in the presence of initial correlations.

Recently, the open-system dynamics of two qubits has been experimentally investigated in all-optical settings, where the system is represented by the polarization degrees of freedom and the environment by the spectral [10] or by the momentum [11] degrees of freedom. In this paper, we provide an experimental proof of the feasibility and effectiveness of the above-mentioned theoretical scheme for the detection of correlations, observing the effect of initial system-environment correlations in the subsequent open-system dynamics by means of the trace distance. In particular, we show an increase of the trace distance between two reduced states, sharing the same initial environmental state, over its initial value on both short- and long-time scales. Despite the fact that a full tomographic analysis can be performed, thus showing that the experimental setup can cope with the most general situation, the growth of the trace distance can here be detected simply by exploiting visibility data, thus showing that the theoretical analysis can really lead to efficient detection schemes.

The paper is structured as follows: In Sec. II, we briefly present the general theoretical scheme. In Sec. III, we describe the experimental apparatus in some details, whereas in Sec. IV, we describe the use of the spatial light modulator to introduce system-environment correlations, and analyze the evolution of the trace distance. In Sec. V, we provide the full tomographic reconstruction of the state under investigation. Section VI closes the paper with some concluding remarks.

II. UPPER BOUND ON TRACE-DISTANCE EVOLUTION

The trace distance between two quantum states ρ^1 and ρ^2 is defined as

$$D(\rho^1,\rho^2) = \frac{1}{2}\mathrm{Tr}|\rho^1 - \rho^2| = \frac{1}{2}\sum_k |x_k|, \tag{1}$$

with x_k eigenvalues of the traceless operator $\rho^1 - \rho^2$, and its physical meaning lies in the fact that it provides a measure for the distinguishability between two quantum states [12]. It is a metric on the space of physical states, so that for any pair of states ρ^1 and ρ^2, it holds $0 \leqslant D(\rho^1,\rho^2) \leqslant 1$. Every CPT map Λ is a contraction for this metric: $D(\Lambda\rho^1,\Lambda\rho^2) \leqslant D(\rho^1,\rho^2)$, a property which will be crucial in the following analysis.

The dynamics of an open quantum system can be characterized by investigating the dynamics of the trace distance between a pair of reduced states $\rho_S^1(t)$ and $\rho_S^2(t)$, which evolve from two different initial total states $\rho_{SE}^1(0)$ and $\rho_{SE}^2(0)$. The change in the distinguishability between two reduced states can be interpreted as an information flow between the open system and the environment [13]. Indeed, since the reduced states $\rho_S^k(t)$ are obtained from the corresponding initial total states $\rho_{SE}^k(0)$ $k = 1,2$ through the composition of a unitary operation and the partial trace, the contractivity under CPT maps implies that

$$D\big(\rho_S^1(t),\rho_S^2(t)\big) - D\big(\rho_S^1(0),\rho_S^2(0)\big) \leqslant I_{12}(0)\,, \tag{2}$$

where

$$I_{12}(0) \equiv D\big(\rho_{SE}^1(0),\rho_{SE}^2(0)\big) - D\big(\rho_S^1(0),\rho_S^2(0)\big)\,. \tag{3}$$

*andrea.smirne@unimi.it
†davide.brivio@unimi.it
‡simone.cialdi@mi.infn.it
§bassano.vacchini@mi.infn.it
‖matteo.paris@fisica.unimi.it

That is, the increase of the trace distance during the time evolution is bounded from above by the quantity $I_{12}(0)$, which represents the information initially residing outside the open system [9]. It is important to notice that the bound $I_{12}(0)$ can also qualitatively reproduce nontrivial features of the trace-distance dynamics even if it is far from being reached [14]. If the initial total states are uncorrelated and with the same environmental state, i.e., $\rho^1_{SE}(0) = \rho^1_S(0) \otimes \rho_E(0)$ and $\rho^2_{SE}(0) = \rho^2_S(0) \otimes \rho_E(0)$, then $I_{12}(0) = 0$. Thus, for identical environmental states, one can find an increase of the trace distance

$$D\big(\rho^1_S(t), \rho^2_S(t)\big) > D\big(\rho^1_S(0), \rho^2_S(0)\big)$$

at a time t only if some correlations are present in at least one of the two initial total states.

III. EXPERIMENTAL SETUP

In our all-optical experimental setup, the total system under investigation consists of a two-photon state produced by spontaneous parametric down conversion. We look at the evolution of the two-qubit polarization entangled state, which represents the reduced system, and trace out the momentum degrees of freedom, which are not observed and represent the environment. We exploit a programmable spatial light modulator (SLM) to impose an arbitrary polarization- and position-dependent phase shift to the total state. A linear phase is set both on signal and idler beams in order to purify the state [15], whereas an additional, generic phase function may be imposed to introduce initial correlations between the polarization and the momentum degrees of freedom in a very general way. A further linear phase is then used as a time-evolution parameter for the two-qubit state.

The experimental setup is shown in Fig. 1. A linearly polarized cw, 405 -nm diode laser (Newport LQC405-40P) passes through two cylindrical lenses, which compensate beam astigmatism, then a spatial filter (SF) selects a Gaussian spatial profile and a telescopic system prepares a collimated beam with beam radius of 550 μm. A couple of 1-mm beta-barium borate (S) crystals, cut for type-I down conversion, with optical axis aligned in perpendicular planes, are used as a source of couples of polarization and momentum entangled photons [16,17]. The process preserves the total energy and the transverse momentum. The half-wave plate (H) set on the pump path rotates the pump polarization in order to balance the

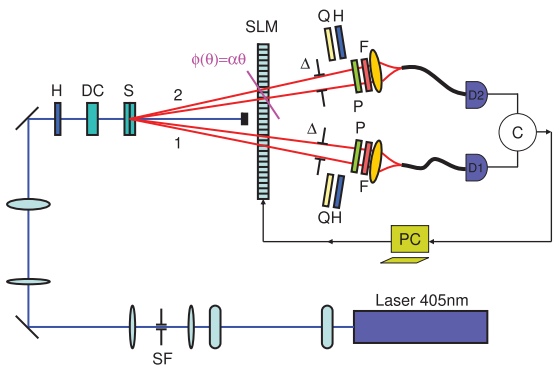

FIG. 1. (Color online) Diagram of the experimental setup.

probability amplitudes of generating a $|VV\rangle$ couple of photons in the first crystal or an $|HH\rangle$ couple in the second one. The couples are generated around a central angle of $\pm 3^\circ$ and we select $\Delta = 10$ mrad with two slits set on signal (2) and idler (1) paths. Two long-pass filters (F) with cut-on wavelength of 780 nm set behind the couplers are used to reduce the background and to select about 60 nm around the central wavelength 810 nm, while the two polarizers (P) are used to perform visibility measurements as explained later on. The delay time between the probability amplitudes of generating a $|VV\rangle$ couple in the first crystal or an $|HH\rangle$ couple in the second crystal reduces the purity of the state. A nonlinear crystal (DC) with the proper length and angle is set on the pump path and precompensates this temporal delay [18–22]. At first order, a linear position-dependent phase shift on both channels between $|HH\rangle$ and $|VV\rangle$ photons arises from the angle-dependent optical path followed by $|VV\rangle$ photons which must traverse the second crystal [19].

IV. SYSTEM-ENVIRONMENT CORRELATIONS AND TRACE-DISTANCE EVOLUTION

A. Theoretical description of the experiment

In our scheme, the SLM performs two basic tasks. First, it allows us to engineer the initial state by the introduction of an arbitrary phase $f(\theta)$. Aside from this, it provides the effective system-environment interaction term sensitive to both the polarization and the momentum degrees of freedom through the introduction of a linear phase $\alpha\theta$, where α is the time-evolution parameter. The total system-environment state is thus given by

$$|\psi_{SE}(\alpha)\rangle = \frac{1}{\sqrt{2}} \int d\theta\, d\theta' g(\theta) g(\theta') (|H\theta\rangle |H\theta'\rangle + e^{i(\alpha\theta + f(\theta))} |V\theta\rangle |V\theta'\rangle). \quad (4)$$

The factorized form $g(\theta)g(\theta')$ is justified by the large spectral distribution [11]. Moreover, $g(\theta)$ is a Gaussian-type shape function with full width at half maximum (FWHM) of 6 mrad. Because of the phase $f(\theta)$, the state in Eq. (4) is correlated, i.e.,

$$\rho_{SE}(\alpha) = |\psi_{SE}(\alpha)\rangle\langle\psi_{SE}(\alpha)| \neq \rho_S(\alpha) \otimes \rho_E(\alpha),$$

and this is true also for the initial total state, i.e., for $\alpha = 0$. Upon tracing out the momentum degrees of freedom, the polarization state is given by

$$\rho_S(\alpha) = \tfrac{1}{2}(|HH\rangle\langle HH| + \epsilon(\alpha)|VV\rangle\langle HH| + \epsilon^*(\alpha)|HH\rangle\langle VV| + |VV\rangle\langle VV|), \quad (5)$$

where

$$\epsilon(\alpha) = \int d\theta |g(\theta)|^2 e^{i[\alpha\theta + f(\theta)]}.$$

Since the angular distribution $g(\theta)$ is symmetric and we use odd functions $f(\theta)$, the quantity $\epsilon(\alpha)$ is real and it equals the interferometric visibility $V(\alpha) = \mathrm{Re}[\epsilon(\alpha)]$.

In order to characterize the effect of the initial system-environment correlations via the trace distance, we have to monitor the evolution of two different polarization states obtained from two different initial total states having the same

environmental state. We compare an initially uncorrelated state $\rho^1_{SE}(\alpha)$, corresponding to Eq. (4) for $f(\theta) = 0$, with an initially correlated state $\rho^2_{SE}(\alpha)$ for a nontrivial function $f(\theta)$. In this way, the reduced system states $\rho^k_S(\alpha)$ $k = 1,2$ are both of the form given by Eq. (5), with different $\epsilon_k(\alpha)$. Note that the product state $\rho^1_{SE}(0)$ differs from $\rho^2_S(0) \otimes \rho^2_E(0)$ only for an overall phase term in the integration over θ, which has no observable consequences on the dynamics of the polarization degrees of freedom. The trace distance between the two reduced states under investigation is then given by

$$D\left(\rho^1_S(\alpha),\rho^2_S(\alpha)\right) = \frac{1}{2}\,|\epsilon_1(\alpha) - \epsilon_2(\alpha)| = \frac{1}{2}\left|\int d\theta |g(\theta)|^2 e^{i\alpha\theta}(1 - e^{if(\theta)})\right|. \quad (6)$$

Different choices for the initial phase $f(\theta)$ result in different dynamical behavior of the trace distance. We have exploited this fact to analyze in detail the effect of initial system-environment correlations on the subsequent evolution of the open system.

B. Experimental results

Experimentally, we have measured the quantity $\epsilon(\alpha)$ for $f(\theta) = 0$ and $f(\theta) = \sin(\lambda\theta)$, exploiting its equality with the visibility, obtained in the standard way by counting the coincidences with polarizers set at 45°,45° and at 45°, -45° (see [20] for further details). The functions of the variable θ are discretized by the SLM and thus become functions of the pixel number n. The resolution is given by h/D, where $h = 100$ μm is the pixel width and $D = 330$ mm is the SLM distance from the source. In our experiment, the SLM introduces the functions

$$\phi^1(n) = -a_{\rm opt}(n - n_1) + b, \qquad \phi^2(n,a) = a_{\rm opt}(n - n_2) + a(n - n_2) + f(n - n_2) \quad (7)$$

on the two beams, respectively, where $a_{\rm opt} = 0.1$ rad/pixel is an optimal slope used to achieve the maximal purification of the polarization entangled state, and the constant b is used to offset the residual constant term. The integers n_1 and n_2 are the central pixel numbers on the idler and on the signal beams. The experimental evolution parameter is then $a = \alpha h/D$ and is expressed in rad/pixel.

The trace distance is the quantity that reveals the presence and the effects of initial correlations, and its behavior is reported in Fig. 2, together with the visibility that provides the raw data from which the trace distance can be extracted in the present case. In the figure, full circles describe the trace distance, as a function of the evolution parameter a, between the reduced state $\rho^1_S(a)$ evolved from the initial total product state, i.e., $f(n - n_2) = 0$, and the reduced state $\rho^2_S(a)$ related to the initial correlated state with $f(n - n_2) = \sin[\lambda(n - n_2)]$. The trace distance, after an initial decrease and a first small oscillation, presents a revival up to a value that is more than three times the initial one. As expected, the reduced system can access information, which is initially outside it, related to its initial correlations with the environment. The trace distance reaches its maximum around $a = 0.6$ rad/pixel, toward the end of the monitored time interval. The maximum of the trace distance quantifies the total amount of information that can be accessed by means of measurements performed on the reduced system only [14]. Note that it can be shifted to smaller values of the evolution parameter a by decreasing the absolute value of λ. Thus, by introducing a sinusoidal phase modulation via the SLM, we have obtained a behavior of the trace distance that highlights the presence of initial correlations and their effects in the subsequent evolution, also for long times [23].

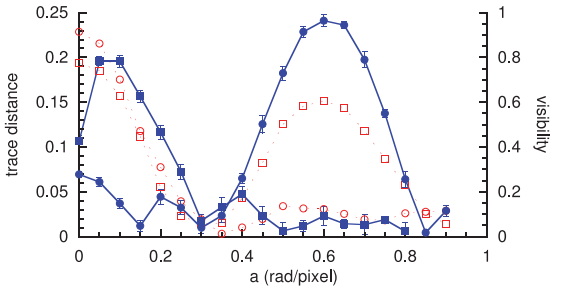

FIG. 2. (Color online) Trace distance and visibility as a function of the experimental evolution parameter a, the two quantities are related through Eq. (6). Full circles describe the trace distance between $\rho^1_S(a)$, i.e., $f(n - n_2) = 0$, and $\rho^2_S(a)$ with $f(n - n_2) = \sin[\lambda(n - n_2)]$, $\lambda = -0.6$ rad/pixel. Full squares describe the trace distance between $\rho^1_S(a)$ and $\rho^2_S(a)$ with $f(n - n_2) = \tau(n - n_2)$, $\tau = 0.1$ rad/pixel. Lines are a guide for the eye. Empty circles refer to visibility with the choice $f(n - n_2) = 0$, whereas empty squares refer to the case in which initial correlations are introduced through the phase function $f(n - n_2) = \sin[\lambda(n - n_2)]$. For the visibility, the uncertainties are within the symbols.

The simplest choice for the phase $f(n - n_2)$ in the initially correlated state $\rho^2_{SE}(\alpha)$ is a second linear phase aside from that containing the evolution parameter a, i.e., $f(n - n_2) = \tau(n - n_2)$. Indeed, this corresponds to shift the initially uncorrelated state $\rho^1_{SE}(\alpha)$ forward in time by τ. Then, from the visibility measurement, we can directly obtain the evolution of the trace distance between $\rho^1_S(a)$ and $\rho^2_S(a)$ with $f(n - n_2) = \tau(n - n_2)$. This is represented by full squares in Fig. 2 for $\tau = 0.1$ rad/pixel. In this case, the growth of the distinguishability between the two reduced states starts from the very beginning of the dynamics. As expected, the trace distance increases over its initial value, reaching its maximum value at $a = 0.1$ rad/pixel and decreasing afterward. The subsequent oscillations can be traced back to the finite pixel size. Notice also that by using a linear term, we can not obtain a revival of the trace distance (as in the previous case) over its initial value for high values of a. Since in this case $\rho^2_S(a) = \rho^1_S(a + \tau)$, the full squares in Fig. 2 also describe the evolution of the trace distance between a pair of reduced states occurring at two different points, separated by τ, of the same dynamics starting from the initial total product state given by $\rho^1_{SE}(0)$. From this point of view, the increase over the initial value of the trace distance indicates that the single evolution under investigation is not compatible with a description through a dynamical semigroup Λ_t, which could be introduced, e.g., on the basis of some phenomenological ansatz. Indeed, the semigroup property $\Lambda_{t+\tau} = \Lambda_t\Lambda_\tau$, together with the trace-distance contractivity under CPT maps, would imply $D(\rho^1_S(t),\rho^2_S(t)) = D(\Lambda_t\rho^1_S(0),\Lambda_t\rho^1_S(\tau)) \leqslant$

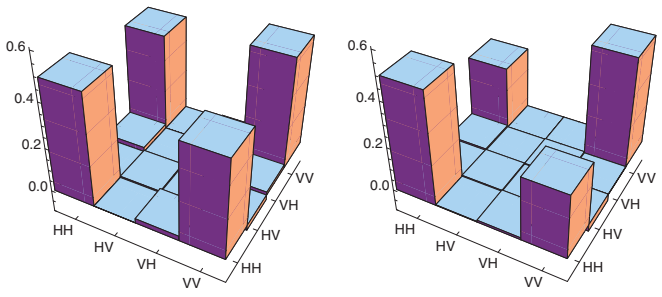

FIG. 3. (Color online) Tomographic reconstruction of the two-qubit density matrix just after the purification (left), without any initial phase, i.e., for $f(n-n_2)=0$ and $a=0$. The visibility is 0.914 ± 0.006. Tomographic reconstruction for $f(n-n_2)=\sin[\lambda(n-n_2)]$ at $a=0.6$ (right), i.e., at the maximum of the visibility revival (compare with Fig. 2). The corresponding visibility is 0.605 ± 0.007.

$D(\rho_s^1(0),\rho_s^1(\tau))=D(\rho_s^1(0),\rho_s^2(0))$. However, in general, one can not discriminate in this way whether the deviations from the semigroup dynamics are due to correlations in the initial total state or to other sources of non-Markovianity [24].

V. STATE RECONSTRUCTION

In order to reconstruct the trace-distance evolution, we only had to perform visibility measurements to access the off-diagonal values $\epsilon_i(\alpha)$. From a mathematical point of view, this corresponds to explicitly determine the projector operator defining the trace distance via the relation $D(\rho^1,\rho^2)=\max_\Pi \mathrm{Tr}\{\Pi(\rho^1-\rho^2)\}$, where the maximum is taken over all the projectors Π or, equivalently, over all the positive operators $\Pi\leqslant\mathbb{1}$. Upon considering the subspace spanned by $\{|HH\rangle,|VV\rangle\}$ and the corresponding σ_x Pauli matrix, the maximum is here obtained from the projectors on the eigenvectors of σ_x, which indeed give back half the difference between the visibilities. However, in more general situations, one could need a full tomographic reconstruction of the reduced states. This would be the case in the presence of nonreal coefficients $\epsilon_k(\alpha)$ in Eqs. (5) and (6) or when dealing with partially or fully unknown states. For this reason, we have also performed state reconstruction by polarization qubit tomography. By means of a quarter-wave plate, a half-wave plate, and a polarizer, we measure a suitable set of independent two-qubit projectors [25,26] and then use the maximum-likelihood reconstruction of the two-qubit polarization density matrix. In Fig. 3 (left), we show the tomographic reconstruction of the polarization state just after the purification and without any initial correlation, i.e., for $f(n-n_2)=0$ and $a=0$. The visibility is 0.914 ± 0.006 (not exactly one mostly because of the large spectrum detected). In Fig. 3 (right), we report the two-qubit tomography for the state characterizing the maximum revival of the visibility in the presence of initial correlations given by $f(n-n_2)=\sin[\lambda(n-n_2)]$, i.e., at $a=0.6$ rad/pixel. The corresponding visibility is 0.605 ± 0.007.

VI. CONCLUSIONS

We have reported an experimental observation of the effect of initial correlations between an open quantum system and its environment by means of the trace distance. In particular, we have shown the increase of the distinguishability between two reduced states, sharing the same reduced environmental state, over its initial value on both short- and long-time scales. Our all-optical scheme is based on the use of a spatial light modulator, which allows us to introduce initial correlations in a very general way. In particular, this setup allows us to engineer different kinds of dynamical behavior of the trace distance, so that one can, e.g., tune the position and the amplitude of the revival points of the distinguishability.

Note added in proof. Recently, we became aware of [27], where initial correlations between the polarization and the spectral degrees of freedom of single-photon states are experimentally witnessed by means of the trace distance.

ACKNOWLEDGMENTS

A.S. and B.V. acknowledge financial support by MIUR, under PRIN2008. The authors thank H.-P. Breuer, E.-M. Laine, S. Maniscalco, and J. Piilo for useful discussions.

[1] H.-P. Breuer and F. Petruccione, *The Theory of Open Quantum Systems* (Oxford University Press, Oxford, 2007).
[2] P. Pechukas, Phys. Rev. Lett. **73**, 1060 (1994); R. Alicki, *ibid.* **75**, 3020 (1995); P. Pechukas, *ibid.* **75**, 3021 (1995).
[3] A. Royer, Phys. Rev. Lett. **77**, 3272 (1996).
[4] P. Štelmachovič and V. Bužek, Phys. Rev. A **64**, 062106 (2001).
[5] T. F. Jordan, A. Shaji, and E. C. G. Sudarshan, Phys. Rev. A **70**, 052110 (2004).
[6] P. Aniello, A. Kossakowski, G. Marmo, F. Ventriglia, and P. Vitale, Open Syst. Inf. Dyn. **17**, 21 (2010).
[7] A. G. Dijkstra and Y. Tanimura, Phys. Rev. Lett. **104**, 250401 (2010).
[8] C. A. Rodriguez-Rosario, K. Modi, A. Kuah, A. Shaji, and E. C. G. Sudarshan, J. Phys. A: Math. Gen. **41**, 205301 (2008); A. Shabani and D. A. Lidar, Phys. Rev. Lett. **102**, 100402 (2009).
[9] E. M. Laine, J. Piilo, and H.-P. Breuer, Europhys. Lett. **92**, 60010 (2010).
[10] Z.-Q. Zhou, C.-F. Li, G. Chen, J.-S. Tang, Y. Zou, M. Gong, and G.-C. Guo, Phys. Rev. A **81**, 064302 (2010).
[11] S. Cialdi, D. Brivio, E. Tesio, and M. G. A. Paris, Phys. Rev. A **83**, 042308 (2011).
[12] C. A. Fuchs and J. van de Graaf, IEEE Trans. Inf. Theory **45**, 1216 (1999).
[13] H.-P. Breuer, E.-M. Laine, and J. Piilo, Phys. Rev. Lett. **103**, 210401 (2009); E.-M. Laine, J. Piilo, and H.-P. Breuer, Phys. Rev. A **81**, 062115 (2010).
[14] A. Smirne, H.-P. Breuer, J. Piilo, and B. Vacchini, Phys. Rev. A **82**, 062114 (2010).
[15] S. Cialdi, D. Brivio, and M. G. A. Paris, Phys. Rev. A **81**, 042322 (2010); Appl. Phys. Lett. **97**, 041108 (2010).

[16] L. Hardy, Phys. Lett. A **161**, 326 (1992).
[17] P. G. Kwiat, E. Waks, A. G. White, I. Appelbaum, and P. H. Eberhard, Phys. Rev. A **60**, R773 (1999).
[18] S. Cialdi, F. Castelli, I. Boscolo, and M. G. A. Paris, Appl. Opt. **47**, 1832 (2008).
[19] R. Rangarajan, M. Goggin, and P. Kwiat, Opt. Express **17**, 18920 (2009).
[20] S. Cialdi, F. Castelli, and M. G. A. Paris, J. Mod. Opt. **56**, 215 (2009).
[21] M. Barbieri, C. Cinelli, F. De Martini, and P. Mataloni, Laser Phys. **16**, 1439 (2006).
[22] G. Brida, M. Genovese, M. V. Chekhova, and L. A. Krivitsky, Phys. Rev. A **77**, 015805 (2008).
[23] J. Dajka and J. Łuczka, Phys. Rev. A **82**, 012341 (2010).
[24] A. R. Usha Devi, A. K. Rajagopal, and Sudha, Phys. Rev. A **83**, 022109 (2011).
[25] K. Banaszek, G. M. D'Ariano, M. G. A. Paris, and M. F. Sacchi, Phys. Rev. A **61**, 010304(R) (1999).
[26] D. F. V. James, P. G. Kwiat, W. J. Munro, and A. G. White, Phys. Rev. A **64**, 052312 (2001).
[27] C.-F. Li, J.-S. Tang, Y.-L. Li, and G.-C. Guo, Phys. Rev. A **83**, 064102 (2011).